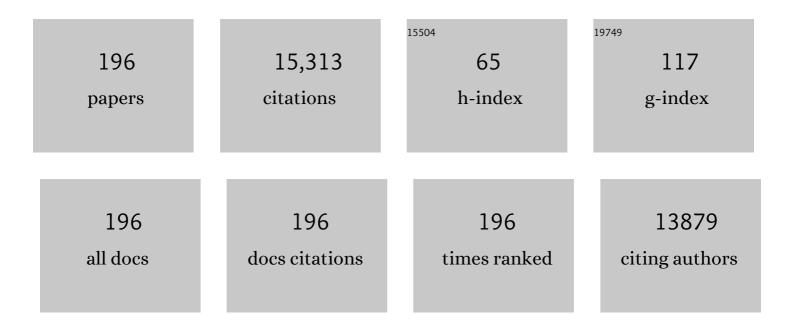
List of Publications by Year in descending order

Source: https://exaly.com/author-pdf/3747440/publications.pdf Version: 2024-02-01



| # | Article | IF | CITATIONS |
|----|---|------|-----------|
| 1 | Mo-O-Bi Bonds as interfacial electron transport bridges to fuel CO2 photoreduction via in-situ reconstruction of black Bi2MoO6/BiO2-x heterojunction. Chemical Engineering Journal, 2022, 429, 132204. | 12.7 | 83 |
| 2 | Porous silver microrods by plasma vulcanization activation for enhanced electrocatalytic carbon dioxide reduction. Journal of Colloid and Interface Science, 2022, 606, 793-799. | 9.4 | 21 |
| 3 | Synergistic effect of isolated Co and Fe dual active sites boosting the photocatalytic hydrogen evolution reaction. Journal of Alloys and Compounds, 2022, 895, 162290. | 5.5 | 20 |
| 4 | Modulating electronic structure of ternary NiMoV LDH nanosheet array induced by doping engineering to promote urea oxidation reaction. Chemical Engineering Journal, 2022, 430, 133100. | 12.7 | 57 |
| 5 | Inherent Facet-Dominant effect for cobalt oxide nanosheets to enhance photocatalytic CO2 reduction. Applied Surface Science, 2022, 578, 151848. | 6.1 | 14 |
| 6 | Ultrathin structure of oxygen doped carbon nitride for efficient CO ₂ photocatalytic reduction. Nanotechnology, 2022, 33, 115404. | 2.6 | 10 |
| 7 | UV-Vis-NIR full-range-responsive carbon-rich carbon nitride nanotubes for enhanced photocatalytic performance. New Journal of Chemistry, 2022, 46, 4654-4665. | 2.8 | 5 |
| 8 | Crystal phase engineering boosted photo-electrochemical kinetics of CoSe2 for oxygen evolution catalysis. Journal of Colloid and Interface Science, 2022, 611, 22-28. | 9.4 | 11 |
| 9 | A bubble-assisted strategy to prepare porous ultrathin carbon nitride for highly-active photocatalytic hydrogen production. Journal of Alloys and Compounds, 2022, 904, 163788. | 5.5 | 12 |
| 10 | Highly efficient photosynthesis of H ₂ O ₂ <i>via</i> two-channel pathway photocatalytic water splitting. Inorganic Chemistry Frontiers, 2022, 9, 1701-1707. | 6.0 | 19 |
| 11 | Self-assembly construction of NiCo LDH/ultrathin g-C3N4 nanosheets photocatalyst for enhanced CO2 reduction and charge separation mechanism study. Rare Metals, 2022, 41, 2118-2128. | 7.1 | 32 |
| 12 | Multidimensional In2O3/In2S3 heterojunction with lattice distortion for CO2 photoconversion. Chinese Journal of Catalysis, 2022, 43, 1286-1294. | 14.0 | 42 |
| 13 | Enhanced photoelectrochemical aptasensing triggered by nitrogen deficiency and cyano group simultaneously engineered 2D carbon nitride for sensitively monitoring atrazine. Biosensors and Bioelectronics, 2022, 206, 114144. | 10.1 | 47 |
| 14 | Activation of Fe species on graphitic carbon nitride nanotubes for efficient photocatalytic ammonia synthesis. International Journal of Energy Research, 2022, 46, 13453-13462. | 4.5 | 3 |
| 15 | Construction of 2D/2D Z-scheme MnO2-x/g-C3N4 photocatalyst for efficient nitrogen fixation to ammonia. Green Energy and Environment, 2021, 6, 538-545. | 8.7 | 38 |
| 16 | Synthesis of carbon nitride in moist environments: A defect engineering strategy toward superior photocatalytic hydrogen evolution reaction. Journal of Energy Chemistry, 2021, 54, 403-413. | 12.9 | 21 |
| 17 | Sulfur promoted n-ï€* electron transitions in thiophene-doped g-C3N4 for enhanced photocatalytic activity. Chinese Journal of Catalysis, 2021, 42, 450-459. | 14.0 | 87 |
| 18 | Large-scale production of ultrathin carbon nitride-based photocatalysts for high-yield hydrogen evolution. Applied Catalysis B: Environmental, 2021, 281, 119475. | 20.2 | 84 |

| # | Article | IF | CITATIONS |
|----|---|------|-----------|
| 19 | Construction 3D rod-like Bi3.64Mo0.36O6.55/CuBi2O4 photocatalyst for enhanced photocatalytic activity via a photo-Fenton-like Cu2+/Cu+ redox cycle. Separation and Purification Technology, 2021, 254, 117546. | 7.9 | 30 |
| 20 | Realizing the synergistic effect of electronic modulation over graphitic carbon nitride for highly efficient photodegradation of bisphenol A and 2-mercaptobenzothiazole: Mechanism, degradation pathway and density functional theory calculation. Journal of Colloid and Interface Science, 2021, 583, 113-127. | 9.4 | 26 |
| 21 | Recent advance in single-atom catalysis. Rare Metals, 2021, 40, 767-789. | 7.1 | 116 |
| 22 | Plasma-induced black bismuth tungstate as a photon harvester for photocatalytic carbon dioxide conversion. New Journal of Chemistry, 2021, 45, 1993-2000. | 2.8 | 11 |
| 23 | Boosting CO ₂ Capture and Its Photochemical Conversion on Bismuth Surface. Physica Status Solidi (A) Applications and Materials Science, 2021, 218, 2000671. | 1.8 | 4 |
| 24 | Metallic rhombohedral NbS2/2D g-C3N4 composite with enhanced photogenerated carriers separation and photocatalytic performance. Applied Surface Science, 2021, 542, 148619. | 6.1 | 14 |
| 25 | Construction of dual ion (Fe3+/Fe2+ and Nb5+/Nb4+) synergy and full spectrum 1D nanorod Fe2O3/NaNbO3 photo-Fenton catalyst for the degradation of antibiotic: Effects of H2O2, S2O82â^' and toxicity. Separation and Purification Technology, 2021, 261, 118269. | 7.9 | 22 |
| 26 | Surface Engineering of 2D Carbon Nitride with Cobalt Sulfide Cocatalyst for Enhanced Photocatalytic Hydrogen Evolution. Physica Status Solidi (A) Applications and Materials Science, 2021, 218, 2100012. | 1.8 | 6 |
| 27 | Minireview on the Commonly Applied Copper-Based Electrocatalysts for Electrochemical CO ₂ Reduction. Energy & Fuels, 2021, 35, 8585-8601. | 5.1 | 20 |
| 28 | Highly sensitive electrochemical immunosensor for the simultaneous detection of multiple tumor markers for signal amplification. Talanta, 2021, 226, 122133. | 5.5 | 26 |
| 29 | Ultrafast electron extraction by 2D carbon nitride modified with CoS cocatalyst for efficient photocatalytic performance. Colloids and Surfaces A: Physicochemical and Engineering Aspects, 2021, 617, 126151. | 4.7 | 14 |
| 30 | Accelerating photocatalytic hydrogen evolution of Ta2O5/g-C3N4 via nanostructure engineering and surface assembly. International Journal of Hydrogen Energy, 2021, 46, 20516-20523. | 7.1 | 11 |
| 31 | Grain-boundary surface terminations incorporating oxygen vacancies for selectively boosting CO2 photoreduction activity. Nano Energy, 2021, 84, 105869. | 16.0 | 43 |
| 32 | Constructing Ni 3 C/2D g 3 N 4 Photocatalyst and the Internal Catalytic Mechanism Study. Physica Status Solidi (A) Applications and Materials Science, 2021, 218, 2100171. | 1.8 | 0 |
| 33 | Unique Dualâ€5ites Boosting Overall CO ₂ Photoconversion by Hierarchical Electron Harvesters. Small, 2021, 17, e2103796. | 10.0 | 38 |
| 34 | Accelerated Photoreduction of CO ₂ to CO over a Stable Heterostructure with a Seamless Interface. ACS Applied Materials & amp; Interfaces, 2021, 13, 39523-39532. | 8.0 | 47 |
| 35 | In Situ Growth and Activation of Ag/Ag ₂ S Nanowire Clusters by H ₂ S Plasma Treatment for Promoted Electrocatalytic CO ₂ Reduction. Advanced Sustainable Systems, 2021, 5, 2100256. | 5.3 | 7 |
| 36 | Exploring deep effects of atomic vacancies on activating CO2 photoreduction via rationally designing indium oxide photocatalysts. Chemical Engineering Journal, 2021, 422, 129888. | 12.7 | 110 |

| # | Article | IF | CITATIONS |
|----|--|------|-----------|
| 37 | Fe atom clusters embedded N-doped graphene decorated with ultrathin mesoporous carbon nitride nanosheets for high efficient photocatalytic performance. Colloids and Surfaces A: Physicochemical and Engineering Aspects, 2021, 629, 127360. | 4.7 | 6 |
| 38 | Nanostructure and functional group engineering of black phosphorus via plasma treatment for CO2 photoreduction. Journal of CO2 Utilization, 2021, 54, 101745. | 6.8 | 13 |
| 39 | Construction of brown mesoporous carbon nitride with a wide spectral response for high performance photocatalytic H ₂ evolution. Inorganic Chemistry Frontiers, 2021, 9, 103-110. | 6.0 | 17 |
| 40 | Self-assembly and boosted photodegradation properties of perylene diimide <i>via</i> different solvents. New Journal of Chemistry, 2021, 45, 21701-21707. | 2.8 | 9 |
| 41 | Emerging surface strategies on graphitic carbon nitride for solar driven water splitting. Chemical Engineering Journal, 2020, 382, 122812. | 12.7 | 155 |
| 42 | Shortâ€ŧime Thermal Oxidation of Ultrathin and Broadband Carbon Nitride for Efficient Photocatalytic H ₂ Generation. ChemCatChem, 2020, 12, 1169-1176. | 3.7 | 7 |
| 43 | Nitrogen-rich graphitic carbon nitride nanotubes for photocatalytic hydrogen evolution with simultaneous contaminant degradation. Journal of Colloid and Interface Science, 2020, 560, 555-564. | 9.4 | 53 |
| 44 | Enhanced photocatalytic H2 evolution by deposition of metal nanoparticles into mesoporous structure of g-C3N4. Colloids and Surfaces A: Physicochemical and Engineering Aspects, 2020, 585, 124067. | 4.7 | 21 |
| 45 | Spatially confined Fe2O3 in hierarchical SiO2@TiO2 hollow sphere exhibiting superior photocatalytic efficiency for degrading antibiotics. Chemical Engineering Journal, 2020, 380, 122583. | 12.7 | 117 |
| 46 | Direct Z-scheme photocatalyst for efficient water pollutant degradation: A case study of 2D g-C3N4/BiVO4. Materials Chemistry and Physics, 2020, 241, 122308. | 4.0 | 38 |
| 47 | Surface amorphous carbon doping of carbon nitride for efficient acceleration of electron transfer to boost photocatalytic activities. Applied Surface Science, 2020, 507, 145145. | 6.1 | 19 |
| 48 | Hierarchical <i>Z</i> -scheme g-C ₃ N ₄ /Au/ZnIn ₂ S ₄ photocatalyst for highly enhanced visible-light photocatalytic nitric oxide removal and carbon dioxide conversion. Environmental Science: Nano, 2020, 7, 676-687. | 4.3 | 79 |
| 49 | Efficient photocatalytic hydrogen evolution by engineering amino groups into ultrathin 2D graphitic carbon nitride. Applied Surface Science, 2020, 507, 145085. | 6.1 | 17 |
| 50 | An all-organic TPA-3CN/2D-C3N4 heterostructure for high efficiency photocatalytic hydrogen evolution. Colloids and Surfaces A: Physicochemical and Engineering Aspects, 2020, 589, 124397. | 4.7 | 10 |
| 51 | Synthesis of Photothermally Stable Triangular Silver Nanoplates for SERS Applications, Photokilling of Bacteria. ChemNanoMat, 2020, 6, 148-153. | 2.8 | 12 |
| 52 | Preparation of a novel sandwich-type electrochemical immunosensor for AFP detection based on an ATRP and click chemistry technique. Polymer Chemistry, 2020, 11, 900-908. | 3.9 | 18 |
| 53 | Plasma treated Bi ₂ WO ₆ ultrathin nanosheets with oxygen vacancies for improved photocatalytic CO ₂ reduction. Inorganic Chemistry Frontiers, 2020, 7, 597-602. | 6.0 | 77 |
| 54 | Nitriding Nickel-Based Cocatalyst: A Strategy To Maneuver Hydrogen Evolution Capacity for Enhanced Photocatalysis. ACS Sustainable Chemistry and Engineering, 2020, 8, 884-892. | 6.7 | 30 |

| # | Article | IF | CITATIONS |
|----|---|------|-----------|
| 55 | Sustainable supercapacitors of nitrogen-doping porous carbon based on cellulose nanocrystals and urea. International Journal of Biological Macromolecules, 2020, 164, 4095-4103. | 7.5 | 31 |
| 56 | Plasma-induced defect engineering: Boosted the reverse water gas shift reaction performance with electron trap. Journal of Colloid and Interface Science, 2020, 580, 814-821. | 9.4 | 29 |
| 57 | An Allâ€Organic Dâ€A System for Visibleâ€Lightâ€Driven Overall Water Splitting. Small, 2020, 16, e2003914. | 10.0 | 80 |
| 58 | Nitrogen-Doped Carbon Quantum Dots from Poly(ethyleneimine) for Optical Dual-Mode Determination of Cu ²⁺ and <scp> </scp> -Cysteine and Their Logic Gate Operation. ACS Applied Materials & Interfaces, 2020, 12, 47245-47255. | 8.0 | 52 |
| 59 | Metal Nanoparticles Confined within an Inorganic–Organic Framework Enable Superior Substrate-Selective Catalysis. ACS Applied Materials & Interfaces, 2020, 12, 42739-42748. | 8.0 | 14 |
| 60 | Solar driven high efficiency hydrogen evolution catalyzed by surface engineered ultrathin carbon nitride. New Journal of Chemistry, 2020, 44, 19314-19322. | 2.8 | 3 |
| 61 | Bowl-shaped graphene oxide/Fe3O4 composites on Au-PCB electrode for electrochemical detection of dopamine. Ionics, 2020, 26, 4171-4181. | 2.4 | 13 |
| 62 | Direct Z-scheme red carbon nitride/rod-like lanthanum vanadate composites with enhanced photodegradation of antibiotic contaminants. Applied Catalysis B: Environmental, 2020, 277, 119245. | 20.2 | 90 |
| 63 | In-situ hydroxyl modification of monolayer black phosphorus for stable photocatalytic carbon dioxide conversion. Applied Catalysis B: Environmental, 2020, 269, 118760. | 20.2 | 147 |
| 64 | Cryo-induced closely bonded heterostructure for effective CO2 conversion: The case of ultrathin BP nanosheets/g-C3N4. Journal of Energy Chemistry, 2020, 49, 89-95. | 12.9 | 49 |
| 65 | Accelerating the Hole Mobility of Graphitic Carbon Nitride for Photocatalytic Hydrogen Evolution via 2D/2D Heterojunction Structural Advantages and Ni(OH) ₂ Characteristic. Solar Rrl, 2020, 4, 1900538. | 5.8 | 28 |
| 66 | Tandem Electrodes for Carbon Dioxide Reduction into C2+ Products at Simultaneously High Production Efficiency and Rate. Cell Reports Physical Science, 2020, 1, 100051. | 5.6 | 60 |
| 67 | Novel broad-spectrum-driven oxygen-linked band and porous defect co-modified orange carbon nitride for photodegradation of Bisphenol A and 2-Mercaptobenzothiazole. Journal of Hazardous Materials, 2020, 396, 122659. | 12.4 | 36 |
| 68 | Crystal phase dependent solar driven hydrogen evolution catalysis over cobalt diselenide. Chemical Engineering Journal, 2020, 396, 125244. | 12.7 | 30 |
| 69 | Preparation and photocatalytic performance of metallic Nb0.9Ta0.1S2/2D-C3N4 composite. Oxford Open Materials Science, 2020, 1, . | 1.8 | 1 |
| 70 | Constructing Schottky junction between 2D semiconductor and metallic nickel phosphide for highly efficient catalytic hydrogen evolution. Applied Surface Science, 2019, 495, 143528. | 6.1 | 35 |
| 71 | Preparation of oxygen-deficient 2D WO3â^'x nanoplates and their adsorption behaviors for organic pollutants: equilibrium and kinetics modeling. Journal of Materials Science, 2019, 54, 12463-12475. | 3.7 | 23 |
| 72 | Efficient photocatalytic hydrogen evolution mediated by defect-rich 1T-PtS ₂ atomic layer nanosheet modified mesoporous graphitic carbon nitride. Journal of Materials Chemistry A, 2019, 7, 18906-18914. | 10.3 | 44 |

Huı Xu

| # | Article | IF | CITATIONS |
|----|---|---------------------|----------------------|
| 73 | Improved chiral electrochemical recognition of tryptophan enantiomers based on threeâ€dimensional molecularly imprinted overoxidized polypyrrole/MnO 2 /carbon felt composites. Chirality, 2019, 31, 917-922. | 2.6 | 6 |
| 74 | Carbon materials from melamine sponges for supercapacitors and lithium battery electrode materials: A review. , 2019, 1, 253-275. | | 135 |
| 75 | 2020 Roadmap on two-dimensional nanomaterials for environmental catalysis. Chinese Chemical Letters, 2019, 30, 2065-2088. | 9.0 | 90 |
| 76 | Tailoring of crystalline structure of carbon nitride for superior photocatalytic hydrogen evolution. Journal of Colloid and Interface Science, 2019, 556, 324-334. | 9.4 | 20 |
| 77 | Graphene quantum dots modified flower like Bi2WO6 for enhanced photocatalytic nitrogen fixation. Journal of Colloid and Interface Science, 2019, 557, 498-505. | 9.4 | 78 |
| 78 | Metal-Oxide-Mediated Subtractive Manufacturing of Two-Dimensional Carbon Nitride for High-Efficiency and High-Yield Photocatalytic H ₂ Evolution. ACS Nano, 2019, 13, 11294-11302. | 14.6 | 109 |
| 79 | Engineering black phosphorus to porous g-C ₃ N ₄ -metal–organic framework membrane: a platform for highly boosting photocatalytic performance. Journal of Materials Chemistry A, 2019, 7, 4408-4414. | 10.3 | 79 |
| 80 | Rapid synthesis of ultrathin 2D materials through liquid-nitrogen and microwave treatments. Journal of Materials Chemistry A, 2019, 7, 5209-5213. | 10.3 | 89 |
| 81 | Cryo-mediated liquid-phase exfoliated 2D BP coupled with 2D C3N4 to photodegradate organic pollutants and simultaneously generate hydrogen. Applied Surface Science, 2019, 490, 117-123. | 6.1 | 26 |
| 82 | 2-Aminopurine modified DNA probe for rapid and sensitive detection of l-cysteine. Talanta, 2019, 202, 520-525. | 5.5 | 6 |
| 83 | Porous nitrogen-rich g-C3N4 nanotubes for efficient photocatalytic CO2 reduction. Applied Catalysis B: Environmental, 2019, 256, 117854. | 20.2 | 271 |
| 84 | Metallic cobalt nanoparticles embedded in sulfur and nitrogen co-doped rambutan-like nanocarbons for the oxygen reduction reaction under both acidic and alkaline conditions. Journal of Materials Chemistry A, 2019, 7, 14291-14301. | 10.3 | 37 |
| 85 | One-step oxygen vacancy engineering of WO3-x/2D g-C3N4 heterostructure: Triple effects for sustaining photoactivity. Journal of Alloys and Compounds, 2019, 795, 426-435. | 5.5 | 42 |
| 86 | Integrating the merits of two-dimensional structure and heteroatom modification into semiconductor photocatalyst to boost NO removal. Chemical Engineering Journal, 2019, 370, 944-951. | 12.7 | 54 |
| 87 | The construction of a Fenton system to achieve in situ H2O2 generation and decomposition for enhanced photocatalytic performance. Inorganic Chemistry Frontiers, 2019, 6, 1490-1500. | 6.0 | 18 |
| 88 | Fabrication of magnetic BaFe ₁₂ O ₁₉ /Ag ₃ PO ₄ composites with an <i>in situ</i> photo-Fenton-like reaction for enhancing reactive oxygen species under visible light irradiation. Catalysis Science and Technology, 2019, 9, 2563-2570. | 4.1 | 30 |
| 89 | Accelerating Photogenerated Charge Kinetics via the Synergetic Utilization of 2D Semiconducting Structural Advantages and Nobleâ€Metalâ€Free Schottky Junction Effect. Small, 2019, 15, e1804613. | 10.0 | 56 |
| 90 | Unveiling the origin of boosted photocatalytic hydrogen evolution in simultaneously (S, P,) Tj ETQq0 0 0 rgBT /C | Dverlock 10 20.2 |) Tf 50 67 Td 300 |

90

6 84-94.

| # | Article | IF | CITATIONS |
|-----|---|------|-----------|
| 91 | Preparation of Co–Mo–O ultrathin nanosheets with outstanding catalytic performance in aerobic oxidative desulfurization. Chemical Communications, 2019, 55, 13995-13998. | 4.1 | 47 |
| 92 | Construction of MnO2/Monolayer g-C3N4 with Mn vacancies for Z-scheme overall water splitting. Applied Catalysis B: Environmental, 2019, 241, 452-460. | 20.2 | 252 |
| 93 | Construction of novel CNT/LaVO4 nanostructures for efficient antibiotic photodegradation. Chemical Engineering Journal, 2019, 357, 487-497. | 12.7 | 158 |
| 94 | Electrochemical Chiral Recognition of Tryptophan Isomers Based on Nonionic Surfactant-Assisted Molecular Imprinting Sol–Gel Silica. ACS Applied Materials & Interfaces, 2019, 11, 2840-2848. | 8.0 | 46 |
| 95 | Integration of metallic TaS ₂ Coâ€catalyst on carbon nitride photoharvester for enhanced photocatalytic performance. Canadian Journal of Chemical Engineering, 2019, 97, 1821-1827. | 1.7 | 1 |
| 96 | Gold nanorods decorated with graphene oxide and multi-walled carbon nanotubes for trace level voltammetric determination of ascorbic acid. Mikrochimica Acta, 2019, 186, 17. | 5.0 | 27 |
| 97 | One-step synthesis of Fe-doped surface-alkalinized g-C3N4 and their improved visible-light photocatalytic performance. Applied Surface Science, 2019, 469, 739-746. | 6.1 | 103 |
| 98 | Highly Efficient Adsorption of Oils and Pollutants by Porous Ultrathin Oxygen-Modified BCN Nanosheets. ACS Sustainable Chemistry and Engineering, 2019, 7, 3234-3242. | 6.7 | 14 |
| 99 | Constructing Pd/2D-C3N4 composites for efficient photocatalytic H2 evolution through nonplasmon-induced bound electrons. Applied Surface Science, 2019, 467-468, 151-157. | 6.1 | 78 |
| 100 | Phase and interlayer effect of transition metal dichalcogenide cocatalyst toward photocatalytic hydrogen evolution: The case of MoSe2. Applied Catalysis B: Environmental, 2019, 243, 330-336. | 20.2 | 105 |
| 101 | Integrating CoOx cocatalyst on hexagonal α-Fe2O3 for effective photocatalytic oxygen evolution. Applied Surface Science, 2019, 469, 933-940. | 6.1 | 48 |
| 102 | Three dimensional polyaniline/MgIn2S4 nanoflower photocatalysts accelerated interfacial charge transfer for the photoreduction of Cr(VI), photodegradation of organic pollution and photocatalytic H2 production. Chemical Engineering Journal, 2019, 360, 1601-1612. | 12.7 | 142 |
| 103 | Construction of 2D SnS2/g-C3N4 Z-scheme composite with superior visible-light photocatalytic performance. Applied Surface Science, 2019, 467-468, 56-64. | 6.1 | 79 |
| 104 | Chemical reduction implanted oxygen vacancy on the surface of 1D MoO3â^'x/g-C3N4 composite for boosted LED light-driven photoactivity. Journal of Materials Science, 2019, 54, 5343-5358. | 3.7 | 36 |
| 105 | Steering charge transfer for boosting photocatalytic H2 evolution: Integration of two-dimensional semiconductor superiorities and noble-metal-free Schottky junction effect. Applied Catalysis B: Environmental, 2019, 245, 477-485. | 20.2 | 64 |
| 106 | In-situ formation of hierarchical 1D-3D hybridized carbon nanostructure supported nonnoble transition metals for efficient electrocatalysis of oxygen reaction. Applied Catalysis B: Environmental, 2019, 243, 151-160. | 20.2 | 66 |
| 107 | Construction of a few-layer g-C3N4/α-MoO3 nanoneedles all-solid-state Z-scheme photocatalytic system for photocatalytic degradation. Journal of Energy Chemistry, 2019, 29, 65-71. | 12.9 | 54 |
| 108 | Comparison of Triangular Silver Nanoprisms with Different Capping Agents and Structural Size for H ₂ O ₂ Etching-Based Biosensors. Nano, 2018, 13, 1850022. | 1.0 | 6 |

| # | Article | IF | CITATIONS |
|-----|--|------|-----------|
| 109 | Graphene quantum dots modified Ag ₃ PO ₄ for facile synthesis and the enhanced photocatalytic performance. Journal of the Chinese Advanced Materials Society, 2018, 6, 255-269. | 0.7 | 8 |
| 110 | Gold/monolayer graphitic carbon nitride plasmonic photocatalyst for ultrafast electron transfer in solar-to-hydrogen energy conversion. Chinese Journal of Catalysis, 2018, 39, 760-770. | 14.0 | 36 |
| 111 | High-Adsorption, Self-Extinguishing, Thermal, and Acoustic-Resistance Aerogels Based on Organic and Inorganic Waste Valorization from Cellulose Nanocrystals and Red Mud. ACS Sustainable Chemistry and Engineering, 2018, 6, 7168-7180. | 6.7 | 68 |
| 112 | 0D/2D Fe2O3 quantum dots/g-C3N4 for enhanced visible-light-driven photocatalysis. Colloids and Surfaces A: Physicochemical and Engineering Aspects, 2018, 541, 188-194. | 4.7 | 54 |
| 113 | Synthesis of PAN copolymer containing pendant 2-ureido-4[1H]-pyrimidone (UPy) units by RAFT polymerization and its adsorption behaviors of Hg2+. Polymer Bulletin, 2018, 75, 4327-4339. | 3.3 | 5 |
| 114 | Electrochemical immunosensor detection of tumor markers based on a GO composite nanoprobe for signal amplification. Analytical Methods, 2018, 10, 526-532. | 2.7 | 14 |
| 115 | An efficient method for the synthesis of a polymer brush via click chemistry and its ultrasensitive electrochemical detection of AFP. Analytical Methods, 2018, 10, 2390-2397. | 2.7 | 4 |
| 116 | Electrochemical CO ₂ Reduction with Atomic Ironâ€Dispersed on Nitrogenâ€Doped Graphene. Advanced Energy Materials, 2018, 8, 1703487. | 19.5 | 369 |
| 117 | 1D metallic MoO2-C as co-catalyst on 2D g-C3N4 semiconductor to promote photocatlaytic hydrogen production. Applied Surface Science, 2018, 447, 732-739. | 6.1 | 69 |
| 118 | Solvothermal synthesis of metallic 1T-WS2: A supporting co-catalyst on carbon nitride nanosheets toward photocatalytic hydrogen evolution. Chemical Engineering Journal, 2018, 335, 282-289. | 12.7 | 161 |
| 119 | Atomic Layered Titanium Sulfide Quantum Dots as Electrocatalysts for Enhanced Hydrogen Evolution Reaction. Advanced Materials Interfaces, 2018, 5, 1700895. | 3.7 | 30 |
| 120 | A green Pickering emulsion stabilized by cellulose nanocrystals via RAFT polymerization. Cellulose, 2018, 25, 77-85. | 4.9 | 31 |
| 121 | Multifunctional nanocomplex for surface-enhanced Raman scattering imaging and near-infrared photodynamic antimicrobial therapy of vancomycin-resistant bacteria. Colloids and Surfaces B: Biointerfaces, 2018, 161, 394-402. | 5.0 | 45 |
| 122 | Constructing magnetic catalysts with in-situ solid-liquid interfacial photo-Fenton-like reaction over Ag3PO4@NiFe2O4 composites. Applied Catalysis B: Environmental, 2018, 225, 40-50. | 20.2 | 175 |
| 123 | Self-assembled synthesis of defect-engineered graphitic carbon nitride nanotubes for efficient conversion of solar energy. Applied Catalysis B: Environmental, 2018, 225, 154-161. | 20.2 | 296 |
| 124 | 2D heterostructure comprised of metallic 1T-MoS2/Monolayer O-g-C3N4 towards efficient photocatalytic hydrogen evolution. Applied Catalysis B: Environmental, 2018, 220, 379-385. | 20.2 | 231 |
| 125 | A multidimensional In ₂ S ₃ –CuInS ₂ heterostructure for photocatalytic carbon dioxide reduction. Inorganic Chemistry Frontiers, 2018, 5, 3163-3169. | 6.0 | 67 |
| 126 | A Specifically Exposed Cobalt Oxide/Carbon Nitride 2D Heterostructure for Carbon Dioxide Photoreduction. Industrial & Engineering Chemistry Research, 2018, 57, 17394-17400. | 3.7 | 76 |

| # | Article | IF | CITATIONS |
|-----|---|--------|-----------|
| 127 | Controllable synthesized heterostructure photocatalyst Mo ₂ C@C/2D g-C ₃ N ₄ : enhanced catalytic performance for hydrogen production. Dalton Transactions, 2018, 47, 14706-14712. | 3.3 | 41 |
| 128 | Graphene oxide-modified LaVO ₄ nanocomposites with enhanced photocatalytic degradation efficiency of antibiotics. Inorganic Chemistry Frontiers, 2018, 5, 2818-2828. | 6.0 | 31 |
| 129 | A novel nanocomposite based on fluorescent turn-on gold nanostars for near-infrared photothermal therapy and self-theranostic caspase-3 imaging of glioblastoma tumor cell. Colloids and Surfaces B: Biointerfaces, 2018, 170, 303-311. | 5.0 | 30 |
| 130 | Synergistic effects of MoO2 nanosheets and graphene-like C3N4 for highly improved visible light photocatalytic activities. Applied Surface Science, 2018, 457, 1142-1150. | 6.1 | 32 |
| 131 | Surface N modified 2D g-C3N4 nanosheets derived from DMF for photocatalytic H2 evolution. Applied Surface Science, 2018, 459, 845-852. | 6.1 | 36 |
| 132 | Multifunctional C-Doped CoFe ₂ O ₄ Material as Cocatalyst to Promote Reactive Oxygen Species Generation over Magnetic Recyclable C–CoFe/Ag–AgX Photocatalysts. ACS Sustainable Chemistry and Engineering, 2018, 6, 11968-11978. | 6.7 | 42 |
| 133 | Electrochemical chiral sensor based on cellulose nanocrystals and multiwall carbon nanotubes for discrimination of tryptophan enantiomers. Cellulose, 2018, 25, 3861-3871. | 4.9 | 27 |
| 134 | Designing Visibleâ€Lightâ€Driven Zâ€scheme Catalyst 2D g ₃ N ₄ /Bi ₂ MoO ₆ : Enhanced Photodegradation Activity of Organic Pollutants. Physica Status Solidi (A) Applications and Materials Science, 2018, 215, 1800520. | 1.8 | 19 |
| 135 | Bio-mediated synthesis and antibacterial activity against aquatic pathogens of silver nanoparticles decorated titania nanosheets in dark and under solar-light irradiation. Materials Technology, 2018, 33, 532-542. | 3.0 | 7 |
| 136 | Highly Efficient Visible-Light-Driven Schottky Catalyst MoN/2D g-C ₃ N ₄ for Hydrogen Production and Organic Pollutants Degradation. Industrial & Engineering Chemistry Research, 2018, 57, 8863-8870. | 3.7 | 35 |
| 137 | Non-metal photocatalyst nitrogen-doped carbon nanotubes modified mpg-C3N4: facile synthesis and the enhanced visible-light photocatalytic activity. Journal of Colloid and Interface Science, 2017, 494, 38-46. | 9.4 | 74 |
| 138 | Transformation from Ag@Ag3PO4 to Ag@Ag2SO4 hybrid at room temperature: preparation and its visible light photocatalytic activity. Journal of Nanoparticle Research, 2017, 19, 1. | 1.9 | 9 |
| 139 | Graphene quantum dots modified mesoporous graphite carbon nitride with significant enhancement of photocatalytic activity. Applied Catalysis B: Environmental, 2017, 207, 429-437. | 20.2 | 238 |
| 140 | Synthesis of novel polymer brushes of poly(acrylonitrile-g-N,Nʹ-dimethylaminoethyl methacrylate) by nitrile modification. Iranian Polymer Journal (English Edition), 2017, 26, 355-364. | 2.4 | 5 |
| 141 | Reversible Formation of gâ€C ₃ N ₄ 3D Hydrogels through Ionic Liquid Activation: Gelation Behavior and Roomâ€Temperature Gasâ€Sensing Properties. Advanced Functional Materials, 2017, 27, 1700653. | 14.9 | 90 |
| 142 | Design of 3D WO ₃ /h-BN nanocomposites for efficient visible-light-driven photocatalysis. RSC Advances, 2017, 7, 25160-25170. | 3.6 | 31 |
| 143 | High Efficiency Photocatalytic Water Splitting Using 2D αâ€Fe ₂ 0 ₃ /gâ€C ₃ N ₄ Zâ€Scheme Catalysts. Advanced Energy Materials, 2017, 7, 1700025. | / 19.5 | 664 |
| 144 | Enhancing reactive oxygen species generation and photocatalytic performance via adding oxygen reduction reaction catalysts into the photocatalysts. Applied Catalysis B: Environmental, 2017, 218, 174-185. | 20.2 | 82 |

| # | Article | IF | CITATIONS |
|-----|---|------|-----------|
| 145 | Designing Zâ€scheme 2D ₃ N ₄ /Ag ₃ VO ₄ hybrid structures for improved photocatalysis and photocatalytic mechanism insight. Physica Status Solidi (A) Applications and Materials Science, 2017, 214, 1600946. | 1.8 | 18 |
| 146 | Construction of SnO ₂ /graphene-like g-C ₃ N ₄ with enhanced visible light photocatalytic activity. RSC Advances, 2017, 7, 36101-36111. | 3.6 | 59 |
| 147 | Construction and preparation of novel 2D metal-free few-layer BN modified graphene-like g-C ₃ N ₄ with enhanced photocatalytic performance. Dalton Transactions, 2017, 46, 11250-11258. | 3.3 | 54 |
| 148 | Hydrothermal synthesis of mpg-C ₃ N ₄ and Bi ₂ WO ₆ nest-like structure nanohybrids with enhanced visible light photocatalytic activities. RSC Advances, 2017, 7, 38682-38690. | 3.6 | 73 |
| 149 | Metallic 1T-TiS ₂ nanodots anchored on a 2D graphitic C ₃ N ₄ nanosheet nanostructure with high electron transfer capability for enhanced photocatalytic performance. RSC Advances, 2017, 7, 55269-55275. | 3.6 | 12 |
| 150 | Cryo-mediated exfoliation and fracturing of layered materials into 2D quantum dots. Science Advances, 2017, 3, e1701500. | 10.3 | 91 |
| 151 | Mercury detection based on label-free and isothermal enzyme-free amplified fluorescence platform. Talanta, 2017, 162, 368-373. | 5.5 | 13 |
| 152 | Enhancing charge density and steering charge unidirectional flow in 2D non-metallic semiconductor-CNTs-metal coupled photocatalyst for solar energy conversion. Applied Catalysis B: Environmental, 2017, 202, 112-117. | 20.2 | 71 |
| 153 | Facile One-Pot Green Synthesis and Antibacterial Activities of GO/Ag Nanocomposites. Acta Metallurgica Sinica (English Letters), 2017, 30, 36-44. | 2.9 | 19 |
| 154 | Biogenic synthesis of silver nanoparticles using ginger (Zingiber officinale) extract and their antibacterial properties against aquatic pathogens. Acta Oceanologica Sinica, 2017, 36, 95-100. | 1.0 | 54 |
| 155 | Construction of a 2D Grapheneâ€Like MoS ₂ /C ₃ N ₄ Heterojunction with Enhanced Visibleâ€Light Photocatalytic Activity and Photoelectrochemical Activity. Chemistry - A European Journal, 2016, 22, 4764-4773. | 3.3 | 149 |
| 156 | PMDETA as an efficient catalyst for bulk reversible complexation mediated polymerization (RCMP) in the absence of additional metal salts and deoxygenation. RSC Advances, 2016, 6, 97455-97462. | 3.6 | 19 |
| 157 | Ultrasonic-assisted pyrolyzation fabrication of reduced SnO2–x /g-C3N4 heterojunctions: Enhance photoelectrochemical and photocatalytic activity under visible LED light irradiation. Nano Research, 2016, 9, 1969-1982. | 10.4 | 67 |
| 158 | Exonuclease III assisted and label-free detection of mercury ion based on toehold strand displacement amplification strategy. Analytical Methods, 2016, 8, 7054-7060. | 2.7 | 7 |
| 159 | WO ₃ nanorod photocatalysts decorated with few-layer g-C ₃ N ₄ nanosheets: controllable synthesis and photocatalytic mechanism research. RSC Advances, 2016, 6, 80193-80200. | 3.6 | 17 |
| 160 | A silver on 2D white-C3N4support photocatalyst for mechanistic insights: synergetic utilization of plasmonic effect for solar hydrogen evolution. RSC Advances, 2016, 6, 112420-112428. | 3.6 | 30 |
| 161 | Oxygenated monolayer carbon nitride for excellent photocatalytic hydrogen evolution and external quantum efficiency. Nano Energy, 2016, 27, 138-146. | 16.0 | 379 |
| 162 | Preparation of corn stalk-based adsorbents and their specific application in metal ions adsorption. Chemical Papers, 2016, 70, . | 2.2 | 12 |

| # | Article | IF | CITATIONS |
|-----|--|------|-----------|
| 163 | Template-free synthesis of 2D porous ultrathin nonmetal-doped g-C 3 N 4 nanosheets with highly efficient photocatalytic H 2 evolution from water under visible light. Applied Catalysis B: Environmental, 2016, 187, 144-153. | 20.2 | 415 |
| 164 | BN nanosheets modified WO 3 photocatalysts for enhancing photocatalytic properties under visible light irradiation. Journal of Alloys and Compounds, 2016, 660, 48-54. | 5.5 | 55 |
| 165 | Three-dimensionally ordered macroporous WO 3 modified Ag 3 PO 4 with enhanced visible light photocatalytic performance. Ceramics International, 2016, 42, 1392-1398. | 4.8 | 27 |
| 166 | Iron-mediated activators generated by electron transfer for atom-transfer radical polymerization of methyl methacrylate using ionic liquid as ligand and Fe(0) wire as reducing agent. Polymer International, 2015, 64, 1754-1761. | 3.1 | 4 |
| 167 | Magnetic g-C ₃ N ₄ /NiFe ₂ O ₄ hybrids with enhanced photocatalytic activity. RSC Advances, 2015, 5, 57960-57967. | 3.6 | 110 |
| 168 | Controllable synthesis of CeO ₂ /g-C ₃ N ₄ composites and their applications in the environment. Dalton Transactions, 2015, 44, 7021-7031. | 3.3 | 125 |
| 169 | In-Situ-Reduced Synthesis of Ti ³⁺ Self-Doped TiO ₂ /g-C ₃ N ₄ Heterojunctions with High Photocatalytic Performance under LED Light Irradiation. ACS Applied Materials & Interfaces, 2015, 7, 9023-9030. | 8.0 | 489 |
| 170 | Direct Synthesis of Porous Nanorod‶ype Graphitic Carbon Nitride/CuO Composite from Cu–Melamine Supramolecular Framework towards Enhanced Photocatalytic Performance. Chemistry - an Asian Journal, 2015, 10, 1276-1280. | 3.3 | 131 |
| 171 | One-pot synthesis of copper-doped graphitic carbon nitride nanosheet by heating Cu–melamine supramolecular network and its enhanced visible-light-driven photocatalysis. Journal of Solid State Chemistry, 2015, 228, 60-64. | 2.9 | 140 |
| 172 | Synthesis and characterization of BN/Bi ₂ WO ₆ composite photocatalysts with enhanced visible-light photocatalytic activity. RSC Advances, 2015, 5, 88832-88840. | 3.6 | 41 |
| 173 | Novel visible-light-driven CQDs/Bi 2 WO 6 hybrid materials with enhanced photocatalytic activity toward organic pollutants degradation and mechanism insight. Applied Catalysis B: Environmental, 2015, 168-169, 51-61. | 20.2 | 486 |
| 174 | Synthesis of few-layer MoS ₂ nanosheet-loaded Ag ₃ PO ₄ for enhanced photocatalytic activity. Dalton Transactions, 2015, 44, 3057-3066. | 3.3 | 71 |
| 175 | g-C3N4 modified Bi2O3 composites with enhanced visible-light photocatalytic activity. Journal of Physics and Chemistry of Solids, 2015, 76, 112-119. | 4.0 | 105 |
| 176 | Making Good Use of Food Wastes: Green Synthesis of Highly Stabilized Silver Nanoparticles from Grape Seed Extract and Their Antimicrobial Activity. Food Biophysics, 2015, 10, 12-18. | 3.0 | 51 |
| 177 | Mussel-inspired polydopamine biopolymer decorated with magnetic nanoparticles for multiple pollutants removal. Journal of Hazardous Materials, 2014, 270, 27-34. | 12.4 | 235 |
| 178 | Application of graphene-like layered molybdenum disulfide and its excellent adsorption behavior for doxycycline antibiotic. Chemical Engineering Journal, 2014, 243, 60-67. | 12.7 | 207 |
| 179 | Graphene-analogue carbon nitride: novel exfoliation synthesis and its application in photocatalysis and photoelectrochemical selective detection of trace amount of Cu ²⁺ . Nanoscale, 2014, 6, 1406-1415. | 5.6 | 351 |
| 180 | Nanoscale optical probes for cellular imaging. Chemical Society Reviews, 2014, 43, 2650. | 38.1 | 179 |

| # | Article | IF | CITATIONS |
|-----|--|------|-----------|
| 181 | CNT/Ag3PO4 composites with highly enhanced visible light photocatalytic activity and stability. Chemical Engineering Journal, 2014, 241, 35-42. | 12.7 | 114 |
| 182 | Exfoliated graphene-like carbon nitride in organic solvents: enhanced photocatalytic activity and highly selective and sensitive sensor for the detection of trace amounts of Cu2+. Journal of Materials Chemistry A, 2014, 2, 2563. | 10.3 | 330 |
| 183 | Graphene-analogue boron nitride/Ag ₃ PO ₄ composite for efficient visible-light-driven photocatalysis. RSC Advances, 2014, 4, 56853-56862. | 3.6 | 36 |
| 184 | Celastrol-modified TiO ₂ nanoparticles: effects of celastrol on the particle size and visible-light photocatalytic activity. RSC Advances, 2014, 4, 12098-12104. | 3.6 | 19 |
| 185 | Fabrication of Ti ³⁺ self-doped TiO ₂ (A) nanoparticle/TiO ₂ (R) nanorod heterojunctions with enhanced visible-light-driven photocatalytic properties. RSC Advances, 2014, 4, 37061-37069. | 3.6 | 45 |
| 186 | Preparation of Wheat Straw Matrix- <i>g</i> -Polyacrylonitrile-Based Adsorbent by SET-LRP and Its Applications for Heavy Metal Ion Removal. ACS Sustainable Chemistry and Engineering, 2014, 2, 1843-1848. | 6.7 | 28 |
| 187 | Improving the photocatalytic activity and stability of graphene-like BN/AgBr composites. Applied Surface Science, 2014, 313, 1-9. | 6.1 | 66 |
| 188 | Graphene-based nanoprobes and a prototype optical biosensing platform. Biosensors and Bioelectronics, 2013, 50, 251-255. | 10.1 | 36 |
| 189 | Synthesis and characterization of g-C3N4/MoO3 photocatalyst with improved visible-light photoactivity. Applied Surface Science, 2013, 283, 25-32. | 6.1 | 227 |
| 190 | Highly sensitive recognition of Pb2+ using Pb2+ triggered exonuclease aided DNA recycling. Biosensors and Bioelectronics, 2013, 47, 520-523. | 10.1 | 33 |
| 191 | Visible-light-induced WO3/g-C3N4 composites with enhanced photocatalytic activity. Dalton Transactions, 2013, 42, 8606. | 3.3 | 445 |
| 192 | Novel visible-light-driven AgX/graphite-like C3N4 (X=Br, I) hybrid materials with synergistic photocatalytic activity. Applied Catalysis B: Environmental, 2013, 129, 182-193. | 20.2 | 595 |
| 193 | The CNT modified white C3N4 composite photocatalyst with enhanced visible-light response photoactivity. Dalton Transactions, 2013, 42, 7604. | 3.3 | 226 |
| 194 | Spectroscopic Studies on the Interaction of Vitamin C with Bovine Serum Albumin. Journal of Solution Chemistry, 2009, 38, 15-25. | 1.2 | 63 |
| 195 | Spectroscopic studies on the interaction between nicotinamide and bovine serum albumin. Spectrochimica Acta - Part A: Molecular and Biomolecular Spectroscopy, 2008, 71, 984-988. | 3.9 | 62 |
| 196 | Steering Hole Transfer from the Light Absorber to Oxygen Evolution Sites for Photocatalytic Overall Water Splitting. Advanced Materials Interfaces, 0, , 2101158. | 3.7 | 4 |